

**UNCLASSIFIED**

**AD 4 21998**

**DEFENSE DOCUMENTATION CENTER**

**FOR**

**SCIENTIFIC AND TECHNICAL INFORMATION**

**CAMERON STATION, ALEXANDRIA, VIRGINIA**



**UNCLASSIFIED**

NOTICE: When government or other drawings, specifications or other data are used for any purpose other than in connection with a definitely related government procurement operation, the U. S. Government thereby incurs no responsibility, nor any obligation whatsoever; and the fact that the Government may have formulated, furnished, or in any way supplied the said drawings, specifications, or other data is not to be regarded by implication or otherwise as in any manner licensing the holder or any other person or corporation, or conveying any rights or permission to manufacture, use or sell any patented invention that may in any way be related thereto.

421998

CATALOGED BY DDC  
AS AD NO.

# UPPER LIMITS FOR THE CONTACT ANGLES OF LIQUIDS ON SOLIDS

Elaine G. Shafrin and W. A. Zisman

Surface Chemistry Branch  
Chemistry Division

September 12, 1963

DDC  
REF ID: A6515  
NOV 4 1968



U. S. NAVAL RESEARCH LABORATORY  
Washington, D.C.

## CONTENTS

<b>Abstract</b>	ii
<b>Problem Status</b>	ii
<b>Authorization</b>	ii
<b>INTRODUCTION</b>	<b>1</b>
<b>REFERENCE LIQUIDS</b>	<b>1</b>
<b>SURVEY OF AVAILABLE CONTACT ANGLE DATA</b>	<b>2</b>
<b>THE WETTING OF LOW-ENERGY SURFACES</b>	<b>10</b>
<b>Hydrophobic Behavior</b>	<b>10</b>
Wetting by Methylene Iodide	16
Wetting by n-Hexadecane	17
Wetting by Other Liquids	18
<b>LIMITING WETTING BEHAVIOR</b>	<b>18</b>
<b>REFERENCES</b>	<b>21</b>

## ABSTRACT

Earlier systematic studies of the angle of contact  $\theta$  exhibited by drops of liquid on plane solid surfaces of low surface energy have made data available on equilibrium contact angles. These data were obtained under well-controlled and comparable experimental conditions for many liquids on over 100 different solid surfaces. Examination of the data for eight, selected, pure liquids (water, formamide, methylene iodide, hexachloropropylene, t-butyl naphthalene, dicyclohexyl, n-hexadecane, and n-decane) reveals a wide variation in the wetting behavior of any single liquid toward different solid surfaces. For each liquid, however, graphical plots of cosine  $\theta$  versus the difference in the surface tension  $(\gamma_{LV} - \gamma_s)$  of the pure liquid and the critical surface tension of spreading  $(\gamma_c)$  of the solid are found to group available data into a zone bounded by a straight line passing through the origin ( $\cos \theta = 1, \gamma_{LV} - \gamma_c = 0$ ). From the parameters defining this straight line, estimates can be made of the limiting contact angles for each liquid. These estimates indicate that the maximum possible contact angle for water is  $156^\circ$ , a value of considerable practical as well as theoretical significance, and that for hexadecane is  $109^\circ$ . The largest values of  $\theta$  obtained experimentally are compared with the maximum values of  $\theta$  as an indication of the extent to which actual systems approach these limiting cases.

A rectilinear relation is found between  $\gamma_{LV}$  and the minimum value of  $\gamma_{LV} - \gamma_c$  required for a surface to exhibit a  $90^\circ$  contact angle; extension of this relation to large values of  $\gamma_{LV}$  provides a good fit to the available data for a pure liquid metal, mercury.

## PROBLEM STATUS

This is an interim report; work on this problem is continuing.

## AUTHORIZATION

NRL Problem C02-10  
Subproject RR 001-01-43-4751

Manuscript submitted June 17, 1963.

## UPPER LIMITS FOR THE CONTACT ANGLES OF LIQUIDS ON SOLIDS

### INTRODUCTION

As a result of many investigations of this Laboratory on wetting and the contact angle, reliable data on equilibrium contact angles at 20°C were obtained under comparable and well-controlled experimental conditions for many dozens of pure liquids on over 100 different solid surfaces (1-3). Usually in each past study the primary interest was in the variation of the contact angle among many liquids with respect to a specific solid surface. This paper is the result of an attempt to study how the wetting behavior of specific individual liquids vary with respect to all solid surfaces. More specifically, answers are sought to the following questions about each liquid studied:

1. What is the range of contact angles observed experimentally?
2. What is the effect on the range of contact angles on changing the solid surface composition?
3. What is the maximum contact angle that can be expected for the specified liquid on any solid surface?

### REFERENCE LIQUIDS

Eight pure liquids (water, methylene iodide, formamide, hexachloropropylene, t-butylnaphthalene, dicyclohexyl, n-hexadecane, and n-decane) were chosen for this investigation, with major emphasis concentrated on the data for water, hexadecane, and methylene iodide.

Water is an obvious choice for this investigation because of (a) the importance of the hydrophobic behavior of organic surfaces in science, technology, and the arts, (b) its high surface tension (and the associated large contact angles on many surfaces), and (c) its extremely small molecular size which makes it capable of penetrating adsorbed monolayers as well as many bulk solids. Adam and Elliott (4) have recently demonstrated the water-penetration of polyethylene and polytetrafluoroethylene by contact angle measurements on these surfaces before and after soaking in water. Kawasaki (5) has shown that the variation with time in the water contact angle on paraffin and polymethylmethacrylate could be treated as a problem in the penetration of the solid by diffusion. Our early study of the adsorption of hydrophobic monolayers from aqueous solution (6) emphasized the considerable effect on the contact angle and its hysteresis arising from water retention in the monolayer. Rideal and Tadayon (7) and more recently Gaines (8) and Yiannos (9) have shown that the presence of interstitial water can facilitate overturning of molecules in an adsorbed monolayer, leading to the exposure of the more hydrophilic groups.

Hexadecane was also chosen for this investigation because it is a nonpolar liquid of low surface tension which is incapable of forming hydrogen bonds and it exemplifies a liquid whose cohesive and adhesive properties are in some ways ideally simple since only London dispersion forces are usually involved. Although the large size of the hexadecane molecule makes penetration of molecular pores in bulk solids difficult, its linear structure and molecular flexibility make it able to adlineate with itself or with other molecules containing similar molecular chains as, for example, in an adsorbed monolayer of a polar paraffinic compound.

Methylene iodide was chosen as the third reference liquid because, although it has a high surface tension, it cannot adlineate like hexadecane, and its large size and molecular shape generally preclude permeation into closely packed, adsorbed, organic monolayers. For these reasons it has been much used in the past six years at this Laboratory for studies of the relation between the contact angle and the closeness of packing of adsorbed organic monolayers (10).

Properties of the three liquids of special interest here are compared in Table 1. It will be noted that the liquid surface tension ( $\gamma_{LV}$ ) for these three reference liquids covers almost a threefold range at 20°C. In this same range are the surface tensions at 20°C for the five other liquids, formamide, hexachloropropylene, t-butyl naphthalene, dicyclohexyl, and decane (58.2, 38.1, 33.7, 32.8, and 23.9 dynes/cm, respectively). All eight of these liquids were of high purity, having been freshly purified by the methods detailed previously (22).

Table 1  
Comparison of the Physical Properties of Reference Liquids Investigated

Reference Liquids*	Spatial		Dielectric		Capillary	
	Molecular Volume at 20°C (mol wt/density) (Å³/molecule)	Minimum Effective Cross-sectional Area (Å²/molecule)	Dipole Moment at 20°C (experimental condition) (debyes)	Polarizability (Å³)	Surface Tension at 20°C (dynes/cm)	Spreading Behavior on Clean High-energy Surfaces
Water	30.0 (11)	7†	1.84 (14) (gaseous)	1.48 (15)	72.8 (11)	spreading (20)
Methylene Iodide	133.8 (11)	17†	1.14 (14) (in hexane)	12 (16)	50.8 (18)	nonspreading (10,21)
n-Hexadecane	458.2 (11)	21.3 (12) (liquid) 18.5 (13) (crystal)	0 (14)	30 (17)	27.6 (19)	spreading (20)

\*Numbers in parentheses refer to the References.

†Estimated from Stuart-Briegleb ball models.

#### SURVEY OF AVAILABLE CONTACT ANGLE DATA

All of the contact angles ( $\theta$ ) included in this report are for smooth surfaces and were obtained by slowly advancing a sessile drop of the liquid in order to provide a good approximation to the equilibrium contact angle. The results were free from difficulties with contact angle hysteresis, except where indicated in the original references.

Tables 2 through 4 present a tabulation of the contact angle data for the reference liquids of interest here. These data were principally obtained from published papers in which are to be found full details about the preparation and cleaning of the various solid surfaces. Two types of monolayer-coated surfaces have not been reported previously. Polydimethylsiloxane films were prepared by contacting freshly acid-cleaned "Aloe" glass microscope slides with a  $2.5 \times 10^{-4}$  solution (by weight) of polydimethylsiloxane (DC No. 200; 350 centistokes at 25°C) in benzene for 30 minutes. Following retraction of the solution, the monolayer-coated glass slide was heated for 30 minutes at 220°C. Contact angle measurements made after the slide had cooled to 20°C indicated that the critical surface tension ( $\gamma_c$ ) for spreading on this surface is 24 dynes/cm. Monolayers

**Table 2**  
Wetting Properties of Various Low-Energy Hydrocarbon Surfaces\*

Surface		Critical Surface Tension $\gamma_c$ (dyne/cm)	Contact Angle $\theta$ (degrees)							
Composition	Form†		Water	Formamide	Methylene Iodide	Hexachloro-propylene	tert-Butylnaphthalene	Dicyclo-hexyl	n-Hexadecane	n-Decane
$-CH_3$										
n-Hexatriacontane	XC	21 (25)‡	111	92	77			55		46
Docosylamine	M				69(10)					28
Octadecylamine	M	21.5 (26)‡	101		68					
Octadecylamine	M	22 (27)‡	102	81	66			54		
Octadecylamine	M				69 (10)			47		
Hexadecylamine	M		96 (6)		69 (10)					
Tetradecylamine	M		91 (6)		68 (10)					
Dodecylamine	M		90 (6)		65 (10)					
Undecylamine	M				62 (10)					
Decylamine	M				58 (10)					
Octylamine	M		81 (6)		53 (10)					
Butylamine	M		55 (6)							
Hexacosanoic acid	M				71 (10)					
Docosanoic acid	M		96 (6)		71 (10)					
Eicosanoic acid	M				71 (10)					
Octadecanoic acid	M	21.0 (26)‡		60§	74			57		
Octadecanoic acid	M	21.4 (30)‡			70 (10)				46	30
Hexadecanoic acid	M		83 (6)		70 (10)				47	30
Tetradecanoic acid	M		78 (6)		70 (10)					
Tridecanoic acid	M				67 (10)					
Dodecanoic acid	M		75 (6)		63 (10)					
Decanoic acid	M		70 (6)		59 (10)					
Octanoic acid	M	22.1 (30)‡			57 (10)				45	25
Hexanoic acid	M		64 (6)							
Polydimethylsiloxane	M	23.5‡	101		70			49		36
										13
$-CH_3$ and $-CH_2-$										
Paraffin	B	23 (25)‡	108	91	66			38		27
Hexadecane	L	29 (28)	79					21		7
Dinonylnaphthalene sulfonate (copper soap)	M	29 (32)	82		57					
Octadecylsuccinic acid	M				79 (6)					
Decylsuccinic acid	M				76 (6)					
Octylsuccinic acid	M				73 (6)					
$-CH_2-$										
Polyethylene	P									
Highly crystalline	P									
Lower crystallinity	P	31 (25)	94(33) 94	77	52 (33) 52			7		
Cyclohexylhexanoic acid	M				75 (6)				Spr§	Spr
Cyclohexylbutyric acid	M				74 (6)					
Cyclohexylpropionic acid	M				76 (6)					
Cyclohexylacetic acid	M				52 (6)					
$-CH_2-$ and Phenyl										
Phenylstearic acid	M	28 (34)			55				Spr	
Polystyrene	P	33-35(29)	91	74	35				Spr	
Polystyrene	M	30-35(43)	93	76	§	11	<5		Spr	
Phenyl (edge on)										
Anthracene	XC	25 (28)	94	73						
Naphthalene	XC	25 (28)	95	77						
Naphthalene	XS	25 (28)	92	72						
Phenyl										
$\alpha$ -Naphtholic acid	M	(28)	58					10		
Aniline	M	~(28)	55					5		
Phenylbutyric acid	M		49 (6)		37					
Benzoic acid	M		48 (6)							

\*Numbers in parentheses refer to the References.

†Physical forms are designated as follows: B = bulk; F = film; L = liquid film; M = adsorbed monomolecular layer; XC = single crystal, cleaved; and XS = single crystal, sublimed.

‡Critical surface tension determined by extrapolation to  $\cos \theta = 1$  axis data points for n-alkanes only.

§Attack.

§Spr = liquid spreads ( $\theta = 0^\circ$ ).

## 1

**Table 3**  
Wetting Properties of Various Low-Energy Surfaces Containing Halogen Atoms\*

Composition	Surface	Form†	Critical Surface Tension $\gamma_c$ (dyne/cm)	Contact Angle $\theta$ (degrees)							
				Water	Formamide	Methylene Iodide	Hexachloro-propylene	tert-Butyl-naphthalene	Dicyclo-hexyl	n-Hexa-decane	n-Decane
<b>-CF<sub>3</sub></b>											
MMM methacrylic polymer A with fluorinated side chain	P	10.6 (35)‡	120	110	98	78	79	77	74	74	64
MMM methacrylic polymer S with fluorinated side chain	P	11.1 (35)‡	118	109	97	77	78	76	73	73	64
Perfluorolauric acid	M	5.6 (36)‡	105	103	81	86	84	78	77	77	70
Perfluorocapric acid	M	6.1 (36)‡	102	99	58	77	77	72	72	77	69
Perfluorocapric acid	M	11.0 (37)‡	102	90	94	77	76	74	74	72	62
Perfluorocaprylic acid	M	7.9 (36)‡	102	94	92	76	76	72	72	72	65
Perfluorocapric acid	M	8.6 (36)‡	102	92	74	74	74	71	71	71	64
Perfluorovaleric acid	M	9.0 (36)‡	102	90	74	74	74	71	71	71	62
Perfluorobutyric acid	M	9.2 (36)‡	102	85	68	68	68	70	70	70	61
<b>-CF<sub>3</sub> and -CF<sub>2</sub>‡</b>											
17-(Perfluoroheptyl)-heptadecanoic acid	M	8.0 (24)‡	115	105	101	78	75	75	73	73	63
17-(Perfluoropentyl)-heptadecanoic acid	M	11.4 (24)‡	110	100	94	73	71	71	68	68	58
17-(Perfluoropropyl)-heptadecanoic acid	M	16.4 (24)‡	106	97	86	68	62	62	59	59	48
17-(Perfluoroethyl)-heptadecanoic acid	M	16.0 (24)‡	105	94	83	64	61	61	58	58	46
17-(Perfluoromethyl)-heptadecanoic acid	M	18.4 (26)‡ erratic	32§	73	45	45	60	60	60	60	44
17-(Perfluoromethyl)-heptadecylamine	M	20.0 (26)‡	93	73	53	53	53	50	50	50	34
11-(Perfluorodecyl)-undecanoic acid	M	7.8 (31)‡	118	108	101	79	77	77	75	75	67
11-(Perfluoroheptyl)-undecanoic acid	M	11.7 (31)‡	115	102	98	75	72	72	69	69	58
11-(Perfluorobutyl)-undecanoic acid	M	15.8 (31)‡	108	96	82	68	64	64	62	62	50
11-(Perfluoroethyl)-undecanoic acid	M	18.8 (31)‡	105.	93	79	62	60	60	50	50	35
6-(Perfluorohexyl)-hexanoic acid	M	14.8 (31)‡	114	114	74	74	74	68	68	68	55
<b>-CF<sub>3</sub> and -CF<sub>2</sub>‡</b>											
Polyhexafluoropropylene (HFP) Sample B Samples A,C,D	P	16.2 (38)‡	117		94	70			60	56	47
Copolymers of HFP and poly-tetrafluoroethylene (TFE)											
23% HFP	P	17.8 (39)‡	114		89	64			53	40	
16% HFP	P	18 (39)‡	113		87	66			51	40	
14% HFP	P	18.2 (39)‡	114		86	62			51	39	
11-1/2%HFP	P	- (39)	113		85	61			50	39	
8% HFP	P	18.3 (39)‡	112		84	60			48	37	
6% HFP	P	19.0 (39)‡	110		82	60			46	33	
Perfluoroalkane	L	17 (28)‡							63	49	
<b>-CF<sub>2</sub></b>											
Polytetrafluoroethylene	P	18.5 (22)‡	108	92	88	65	65	65	66	66	38

23% HFP	P	17.8	(39)†	114		89	64			53	40
16% HFP	P	18	(39)†	113		87	66			51	40
14% HFP	P	18.2	(39)†	114		86	62			51	39
11-1/2% HFP	P	-	(39)	113		85	61			50	
8% HFP	P	18.3	(39)†	112		84	60			48	37
6% HFP	P	19.0	(39)†	110		82	60			46	33
Perfluoroalkane	L	17	(28)†							63	49

Polytetrafluoroethylene

P 18.5 (22)† 108 92 88 65 65 65 65 66 46 38

-CF<sub>2</sub>-

-CF<sub>2</sub>H

omega-Monohydroperfluorinated acids	M				88-9(10)						
ψ-Heptadecanoic acid	M				89(10)						
ψ-Pentadecanoic acid	M				89(10)						
ψ-Tridecanoic acid	M	15	(42)†	97	88(10)						
ψ-Unodecanoic acid	M				86-7(10)						
ψ-Nonanoic acid	M										
omega, alpha, alpha-Trihydroperfluorinated alcohols	M				88(10)						
ψ'-Pentadecanol	M				88(10)						
ψ'-Tridecanol	M										

-CF<sub>2</sub>-CFH-

-CF<sub>2</sub>- and -CH<sub>2</sub>-

Polytrifluoroethylene	P	22	(40)	92	76	71		42		37	18
Polyvinylidene fluoride	P	25	(40)	82	59	63					
50:50 Copolymer of TFE and polyethylene	P	26-7 (41)	93	79	69			18		24	
Polyvinyl fluoride	P	28	(40)	80	54	49		39		12	Spr

-CFH-CH<sub>2</sub>-

Polyvinyl fluoride	P	28	(40)	80	54	49		10		Spr	Spr

C, F, Cl

Copolymers of TFE and poly-chlorotrifluoroethylene (Kel-F)											
80:20 TFE:Kel-F (C <sub>10</sub> F <sub>10</sub> Cl)	P	20	(41)	100	91	84			55		37
60:40 TFE:Kel-F (C <sub>10</sub> F <sub>10</sub> Cl <sub>2</sub> )	P	24	(41)	94	75	76			45		Spr
Kel-F	P	31	(41)	90	82	64			18		Spr
Cl(CF <sub>2</sub> -CFCl) <sub>2</sub> CF <sub>2</sub> COOH	M						76-7(10)				27
Cl(CF <sub>2</sub> -CFCl) <sub>2</sub> CF <sub>2</sub> COOH	M						73 (10)				Spr
F <sub>3</sub> C-C=Cl - COOH	M						70 (10)				Spr
HFC-C-F <sub>2</sub> - C=C - COOH	M										

C, H, F, Cl

Polyvinyl chloride	P	39	(40)	87	66	36					
Polyvinylidene chloride	P	40	(40)	80	61	29					

C, Cl

Perchloropentadienoic acid	M	43	(40)	66	32§	34					

C, H, Cl, O, N

3

perfluorinated alcohols ψ'-Pentadecanol ψ'-Tridecanol	M M																			
Polytrifluoroethylene	P	22	(40)	92	76	71				42							37	18		
							-CF <sub>2</sub> - and -CH <sub>2</sub> -													
Polyvinylidene fluoride	P	25	(40)	82	59	63				18							24			
50:50 Copolymer of TFE and polyethylene	P	26-7	(41)	93	79	69				39							12	Spr		
Polyvinyl fluoride	P	28	(40)	80	54	49				10							Spr	Spr		
							C, F, Cl													
Copolymers of TFE and poly-chlorotrifluoroethylene (Kel-F)																				
80:20 TFE:Kel-F (C <sub>10</sub> F <sub>10</sub> Cl)	P	20	(41)	100	91	84				55							37	27		
60:40 TFE:Kel-F (C <sub>10</sub> F <sub>10</sub> Cl <sub>4</sub> )	P	24	(41)	94	75	76				45							Spr	Spr		
Kel-F	P	31	(41)	90	82	64				18							Spr	Spr		
Cl(CF <sub>3</sub> -CFCl) <sub>2</sub> CF <sub>2</sub> COOH	M																			
Cl(CF <sub>3</sub> -CFCl) <sub>2</sub> CF <sub>2</sub> COOH	M																			
F <sub>3</sub> C-C=O-COOH	M																			
	Cl	Cl	Cl																	
HFC <sub>2</sub> CF <sub>2</sub> -C=C-COOH	M																			
	Cl	Cl	Cl																	
							C, H, F, Cl													
Polyvinyl chloride	P	39	(40)	87	66	36														
Polyvinylidene chloride	P	40	(40)	80	61	29														
							C, Cl													
Perchloropentadienoic acid	M	43	(40)	66	32§	34														
							C, H, Cl, O, N													
Copolymer of polyvinylidene chloride with 20% polyacrylonitrile	P	38-44(43)	81	65	27															
							-CH <sub>2</sub> Br													
omega-Monobrominated aliphatic acids	M																			
omega-Bromoundecanoic acid	M																			
omega-Bromomonanoic acid	M																			

\*Numbers in parentheses refer to References.

†Physical forms are designated as follows: L = liquid film; M = adsorbed monomolecular layer; P = polymer.

‡Critical surface tension determined by extrapolation to cos θ = 1 axis the data points for n-alkanes only.

§Attack.

§Spr = liquid spreads ( $\theta=0^\circ$ ).

Table 4  
Wetting Properties of Various Low-Energy Surfaces Containing Oxygen or Nitrogen Atoms\*

Composition	Surface	Form †	Critical Surface Tension $\gamma_c$ (dyne/cm)	Contact Angle $\theta$ (degrees)					
				Water	Formamide	Methylene Iodide	Hexachloro-propylene	Butynaphthalene	Dicyclohexyl n-Hexadecane
C, H, O									
Polymethylmethacrylate	P	39(43)	80	64	41	Spr §	Spr	Spr	Spr
Polyethylene terephthalate	P	43(29)	81	61	38				
Tetradecanedioic acid	M		76(6)						
Dodecanedioic acid	M		65(6)						
Decanedioic (sebacic) acid	M		56(6)						
Hexanedioic (adipic) acid	M		40(6)						
Butanedioic (succinic) acid	M		28(6)						
C, H, O; N									
Polyacrylamide	P		†	†	†	47	Spr	20	19
Pentaerythritol tetranitrate	X								14
110 natural crystal face		40(44)	77	56	41				
101 natural crystal face		45(44)	72	45	31				
Cyclotrimethylene trinitramine	X	44(44)	68	32	30				
Trinitrobutyric acid	M	42(44)	73	35	40				
Nylon 6,6	P	46(29)	70	50	41				

\* Numbers in parentheses refer to References.

† Physical forms are designated as follows: M = absorbed monomolecular layer; P = polymer; X = single crystal.  
‡ Attack.

§ Spr = liquid spreads ( $\theta = 0^\circ$ ).

of selected terminally perfluoroalkyl-substituted undecanoic and hexanoic acids (23) were prepared by adsorption from the melt onto metallographically polished chromium surfaces under conditions identical to those used to prepare films of the terminally perfluoroalkyl-substituted heptadecanoic acids (24).

The contact angle data are most conveniently presented in tabulations based on the atomic composition of the outermost planes of the low-energy solid surfaces as follows:

**Table 2** — Surfaces composed solely of carbon and hydrogen atoms;

**Table 3** — Surfaces containing any halogen atoms (F, Cl, or Br); and

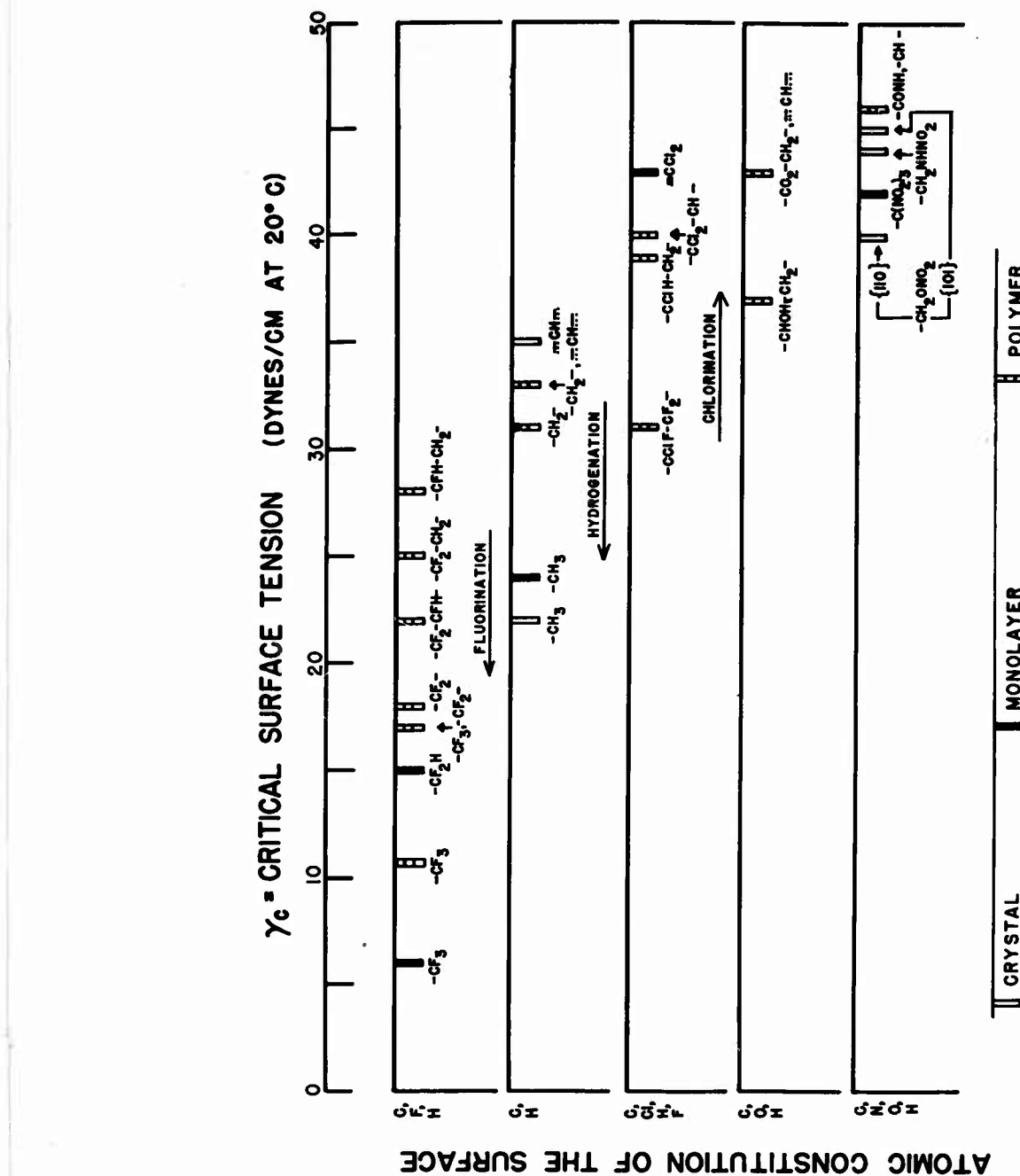
**Table 4** — Surfaces comprising carbon, hydrogen, and oxygen atoms and carbon, hydrogen, oxygen, and nitrogen atoms.

Each table is further divided according to the atomic groupings (e.g., methyl, methylene, etc.) exposed in the surface. The first column (Surface Composition) identifies the surfaces as to bulk chemical composition and the second column (Surface Form) specifies the physical form. Where identical atomic groupings are outermost for several different low-energy surfaces (e.g., the terminal methyl groups exposed in adsorbed monolayers of homologous series of aliphatic derivatives), the surfaces within each atomic-grouping subdivision are listed in the order of their increasing  $\gamma_c$  as listed in the third column (Critical Surface Tension) of each table. In the remaining columns are listed the values of  $\theta$  reported for the reference liquids named in the corresponding column heading. Unless otherwise specified, the contact angle data were obtained from the same reference source as that indicated for  $\gamma_c$ . Also included in these tables are isolated values of  $\theta$  reported for many low-energy surfaces which have not been characterized as to their  $\gamma_c$ .

The largest contact angle exhibited by any of the eight reference liquids on these smooth, clean, low-energy surfaces is  $120^\circ$ , reported for water on a thin coating of a methacrylic ester polymer with perfluorinated side chains (35). The only larger angles reported for any liquids on the surfaces listed in Tables 2-4 are the angles of  $146^\circ$ ,  $150^\circ$ , and  $152^\circ$  observed for mercury on octadecylamine monolayers (27), polytetrafluoroethylene (22), and perfluorodecanoic acid monolayers (37), respectively. The contact angles listed in Tables 2-4 vary from the maximum value of  $120^\circ$  down to the zero angle corresponding to the spreading of the liquid over the surface. In the subsequent discussion of the variation in  $\theta$ , it will be most convenient to relate  $\theta$  to  $\gamma_c$ .

The wide variety of solids for which both reliable equilibrium contact angles and critical surface tensions are available is indicated in Fig. 1, where the legend across the bottom illustrates the differences in physical forms studied and the designation to the left of each line shows the range of atomic compositions. The markers on each line correspond to surfaces exposing only those atoms listed to the left of that line, the specific chemical grouping involved being identified immediately below the appropriate marker. The position of the marker relative to the horizontal scale of critical surface tension values ( $\gamma_c$ ) across the top of the figure indicates the lowest value of  $\gamma_c$  observed for one or more different surfaces exposing the same atomic groupings. For example, the single marker identified as a monolayer exposing  $-CF_3$  groups (upper left in Fig. 1) corresponds in position (at 6 dynes/cm) to the lowest value of  $\gamma_c$  obtained for a group of 15 different fully and partially fluorinated aliphatic acid monolayers (the highest value for the group was less than 19 dynes/cm).

Figure 1 provides a kind of wettability spectrum (2) which allows one to relate  $\gamma_c$  to the surface constitution of over sixty different low-energy surfaces. The lowest values of  $\gamma_c$  are obtained on surfaces comprising C and F atoms only (6 to 19 dynes/cm). On adding H atoms,  $\gamma_c$  increases with increasing hydrogenation (15 to 28 dynes/cm). The next higher range of values is obtained on surfaces comprising only C and H atoms (22 to



35 dynes/cm). Adding halogen atoms other than fluorine to either a C, F or a C, H surface increases  $\gamma_c$ , with a value of 43 dynes/cm being reported for a surface comprising only C and covalent Cl. As a class, the low-energy surfaces with the highest values of  $\gamma_c$  are those exposing either O or N atoms (35 to 45 dynes/cm).

In the following discussion of the variation in wetting of a reference liquid on solid surfaces, it is most convenient to group the surfaces into only four classes (Figs. 2-5), based on the kinds of atoms present:

1. Surfaces exposing any F atoms.
2. Surfaces exposing only C and H atoms.
3. Surfaces exposing halogen atoms but not containing F.
4. Surfaces exposing O or N atoms.

Reference to Fig. 1 shows that these four classes of surfaces are in the order of increasing (although overlapping) critical surface tensions.

## THE WETTING OF LOW-ENERGY SURFACES

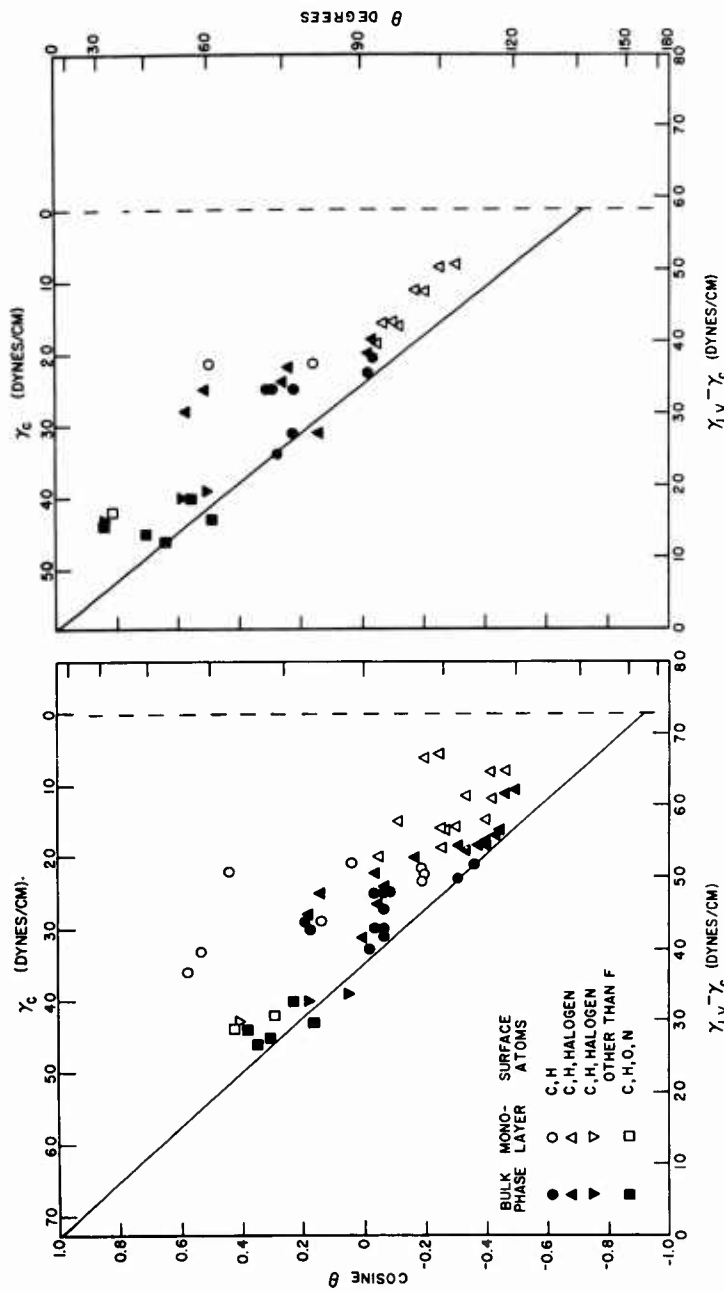
### Hydrophobic Behavior

Reliable equilibrium contact angles of water have been reported for over 100 well-defined, low-energy organic-solid surfaces or adsorption-modified high-energy surfaces (fourth column (Water) of Tables 2-4).

Data on  $\gamma_c$  are also available for at least sixty of these surfaces. The cosine of the hydrophobic contact angle of each surface is conveniently plotted in Fig. 2a against the difference between  $\gamma_{LV}$  of water and  $\gamma_c$  of the solid. All of the data on this figure are for wetting by only one liquid (water). All but nine of the data were obtained at 20°C; however for those nine (all corresponding to bulk polymers exposing only C and F atoms), the contact angles reported (35, 38, 39) were obtained at 25°C. Comparison measurements on polytetrafluoroethylene surfaces at 20° and 25°C indicate that the effect of this small change in temperature on the contact angle does not significantly exceed the experimental error of measurement. Therefore these data are included in Fig. 2a even though only a single value of the surface tension of water is used (72.8 dynes/cm at 20°C). On the same graph one can also plot the values of  $\gamma_c$  decreasing to a zero value toward the right, as shown across the top of the chart. For easy reference, the value of the contact angle is also indicated along the ordinate axis at the right.

Each data point of Fig. 2a represents the hydrophobic behavior of a single solid surface. Symbols of different shapes serve to distinguish the type of solid surfaces according to the composition of their outermost atoms. Filled symbols designate surfaces of bulk organic solids (single crystals, polymers, etc.) and open symbols refer to low-energy surfaces created by adsorption of monomolecular films.

The largest water angle observed is 120° on the  $-CF_3$  rich surface of a thin coating of a polymethacrylic ester having perfluorinated side chains (35); close to this is the 118° angle reported for both a related polymeric surface (an acrylic ester with perfluorinated side chains) (35) and a monolayer of 11-(perfluorododecyl)undecanoic acid adsorbed on a mirror-smooth chromium surface. The group of solid polymers exposing only C and F atoms are represented in Fig. 2a by the filled triangles pointing up. These all have abscissas of 53 dynes/cm or more, since for all such surfaces  $\gamma_c < 20$  dynes/cm. Ten homopolymers and copolymers in this class have been studied and in no instance was the



a. Wetting by water

b. Wetting by formamide

Fig. 2 - Wetting behavior of hydrogen-bonding liquids on low-energy surfaces of varied surface composition

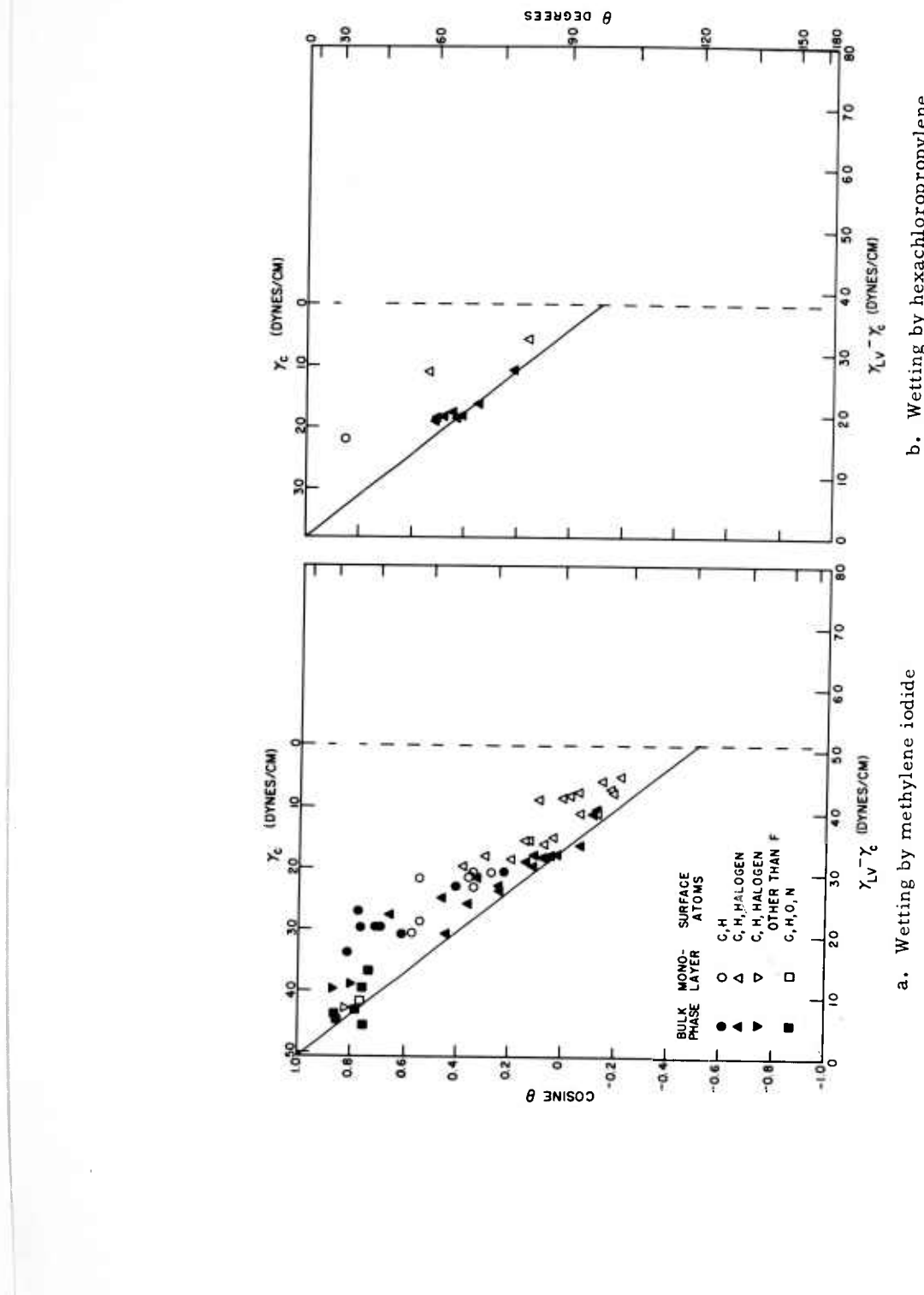
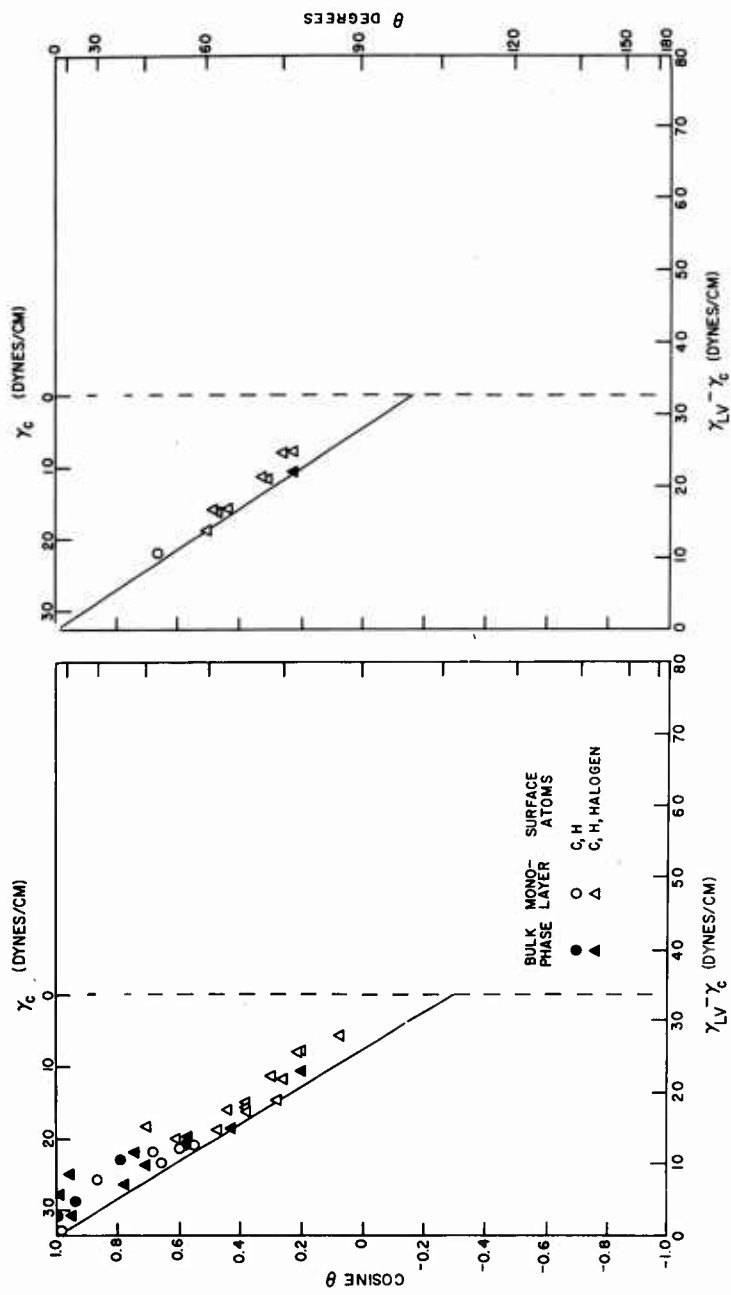


Fig. 3 - Wetting behavior of halocarbons on low-energy surfaces of varied surface composition

a. Wetting by methylene iodide

b. Wetting by hexachloropropylene



a. Wetting by t-butylnaphthalene

b. Wetting by dicyclohexyl

Fig. 4 - Wetting behavior of cyclic hydrocarbons on low-energy surfaces of varied surface composition

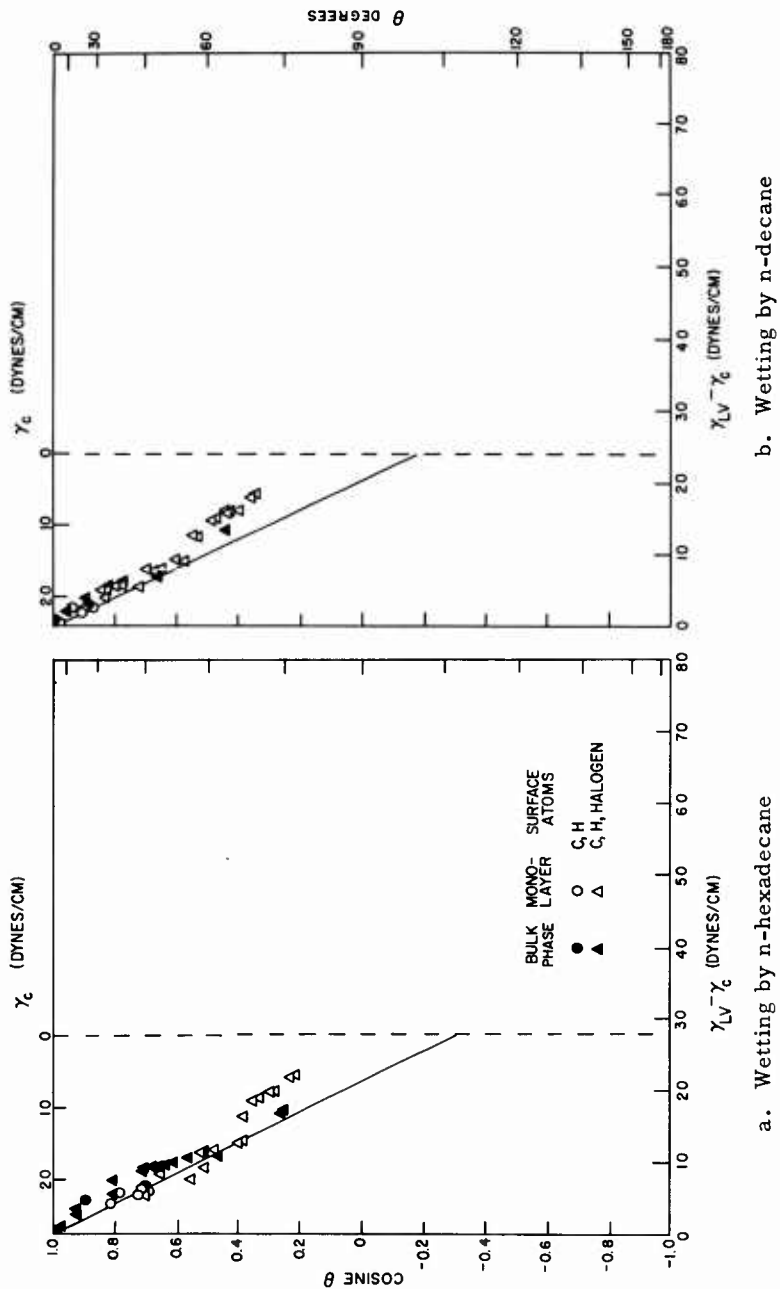


Fig. 5 - Wetting behavior of aliphatic hydrocarbons on low-energy surfaces of varied surface composition

hydrophobic contact angle lower than the  $108^\circ$  value found for polytetrafluoroethylene. Lower hydrophobic angles were invariably obtained when atoms in addition to C and F were introduced in the surfaces (note the ordinates of the remaining filled triangles, pointing up, in Fig. 2a).

The second most hydrophobic class of surfaces is characterized by surfaces composed only of hydrocarbon groups (filled circles of Fig. 2a), but their largest water angles are well below those of the fluorocarbons. In this class, the largest contact angle of  $111^\circ$  is obtained on a cleavage plane of a single crystal of n-hexatriacontane (25), so that it corresponds to a surface comprised only of  $-\text{CH}_3$  groups in the highly condensed packing characteristic of the crystal lattice. Hydrophobic angles of  $108^\circ$  to  $110^\circ$  are common on white paraffin surfaces (25) and undoubtedly these surfaces consist of  $-\text{CH}_2-$  and  $-\text{CH}_3$  groups, the high value of  $\theta$  resulting when there is a high concentration of  $-\text{CH}_3$  groups. Another type of surface exposing  $-\text{CH}_3$  groups is the condensed, adsorbed monolayer of polar paraffinic molecules. The highest water angle observed on such a surface is  $101^\circ$ , the difference between this and  $111^\circ$  reflecting the difference in the closest packing of aliphatic chains obtainable in a system where crystallization is absent. An angle of  $101^\circ$  also is obtained on an adsorbed condensed monolayer of an open-chain polydimethylsiloxane. Since this angle is identical to that reported for the most hydrophobic of the adsorbed aliphatic monolayers, it indicates that the methyl groups exposed by the silicone film are sufficiently close-packed to effectively shield the Si-O linkages from the wetting interface. The water contact angle drops to  $94^\circ$  for a polyethylene surface, paralleling the decrease in  $\theta$  observed between a  $-\text{CF}_3$  and a  $-\text{CF}_2-$  surface previously noted for fluorocarbon surfaces.

Greater water-wettability is observed for those surfaces exposing carbon and halogen atoms other than F (triangular symbols, pointing down). Where the surfaces contain some O and N atoms (square symbols),  $\gamma_c$  is generally characterized by high values and the corresponding data points of Fig. 2a are clustered toward the left-hand portion of the chart. Such surfaces have the lowest hydrophobic contact angles of the bulk organic solids which are not dissolved by or permeable to water molecules; values of  $\theta > 65^\circ$  are the rule. Nevertheless, most of these surfaces are still usefully hydrophobic (cf. nylon 6,6 with a  $70^\circ$  water angle on a surface for which  $\gamma_c = 43$  dynes/cm). The smallest water angle reported on a surface not dissolved by or permeable to molecular water is  $68^\circ$  on a single crystal of cyclotrimethylene trinitramine ( $\gamma_c = 44$  dynes/cm) (45). With solvent action by water, of course, the contact angle drops rapidly, as in the case of polyvinyl alcohol despite the value of  $\gamma_c$  of 37 dynes/cm reported by Ryan et al. (46).

The distribution of the filled and open symbols for surfaces of the same composition indicates that the adsorbed monolayers are generally less hydrophobic than the atomically comparable surfaces of bulk solids. This is a result of the penetration of the surface by water molecules; there may be under some circumstances an added effect caused by the overturning of the polar molecules in the monolayers (7-9). From the distribution of the data points in Fig. 2a it is apparent that  $\cos \theta$  is larger (or  $\theta$  is smaller) the closer  $\gamma_c$  is to  $\gamma_{LV}$ . By definition, any solid surface with  $\gamma_c$  exactly equal to or larger than the  $\gamma_{LV}$  of the liquid will be spread upon by that liquid. Hence, water should spread on any surface having  $\gamma_c > 72.8$  dynes/cm. This is in good agreement with the well-known spreading of water on high-energy surfaces which are free of organic contamination (20).

As  $\gamma_{LV} - \gamma_c$  increases (i.e., as  $\gamma_c$  decreases), the surfaces become more hydrophobic. At larger values of  $\gamma_{LV} - \gamma_c$  the majority of the data points tend to lie within a relatively narrow range of  $\cos \theta$  values and to concentrate toward the lower end of that range. This is surprising since a wider range of water contact angles becomes possible as the difference between  $\gamma_c$  and  $\gamma_{LV}$  is increased. There is no a priori reason why two different surfaces having the same value of  $\gamma_c$  should necessarily exhibit identical water angles.

It is possible to draw an envelope of the minimum  $\cos \theta$  values toward which the data points of Fig. 2a tend to concentrate; when this is done, the envelope is found to be a straight line which originates at the point ( $\cos \theta = 1$ ,  $\gamma_{LV} - \gamma_c = 0$ ). Thus, despite the extreme variations in surface chemical composition and in hydrophobic behavior represented by the data in Fig. 2a, a relation as simple as a straight line adequately represents the minimum  $\cos \theta$  observed experimentally for water. All but two of the data points in Fig. 2a are found to lie on or above this straight line and these two (for polyethylene terephthalate and polyvinyl chloride) also are close. Thus, it becomes possible to predict in advance what the maximum water contact angle can be for a surface having a given value of  $\gamma_c$ ; of course, the actual angle may prove smaller. If a specific water angle is desired (e.g.,  $\theta \geq 90^\circ$  to prevent capillary penetration), the intersection of the limiting line of Fig. 2a with the appropriate ordinate ( $\cos 90^\circ$ ) indicates the smallest difference between  $\gamma_c$  and  $\gamma_{LV}$  for which an angle of  $90^\circ$  is possible. This value of  $\gamma_{LV} - \gamma_c$  is 38.2 dynes/cm, as evident in Fig. 2a. The existence of this minimum difference serves to automatically remove from further consideration any solid surface for which  $\gamma_{LV} - \gamma_c < 38.2$  dynes/cm and, hence, for which  $\gamma_c > 34.6$  dynes/cm. Finally, by extrapolation of this limiting straight line to the maximum possible value of  $\gamma_{LV} - \gamma_c$  (indicated by the vertical dashed line of Fig. 2a), which corresponds to allowing  $\gamma_c$  to approach zero so that  $\gamma_{LV} - \gamma_c$  approaches the value of 72.8 dynes/cm (the surface tension of water), the maximum hydrophobic contact angle possible is indicated to be  $156^\circ$ .

#### Wetting by Methylene Iodide

Although equilibrium contact angle data are available for methylene iodide (Tables 2-4) on a somewhat smaller number of solid surfaces than for water (about 80), they are for almost all of the low-energy surfaces for which  $\gamma_c$  has been measured. Therefore, it is possible to make for methylene iodide a similar plot to Fig. 2a (see Fig. 3a). The largest methylene iodide angle observed experimentally is  $101^\circ$  to  $103^\circ$  on a condensed film of  $-CF_3$  terminal groups; the smallest angle on a surface not dissolved or attacked by the sessile drop is  $29^\circ$  on polyvinylidene chloride ( $\gamma_c = 40$  dynes/cm).

In general, the distribution of data points in Fig. 3a is similar to that of Fig. 2a. The group of low-energy surfaces which exhibits maximum hydrophobicity is also the group having the largest methylene iodide contact angles. Contact angles of  $90^\circ$  or more are common on surfaces consisting of condensed  $-CF_3$  groups, whether bulk organic materials (e.g., polyhexafluoropropylene) or adsorbed monolayers comprising molecules with terminal perfluoroalkyl groups of five or more fluorinated carbon atoms. Condensed monolayers with terminal perfluoroalkyl moieties shorter than this and polymers with significant proportions of  $-CF_2-$  groups exhibit contact angles below  $90^\circ$ . The lowest contact angle reported on any bulk surface comprising only C and F atoms is  $82^\circ$ (39). Methylene iodide contact angles on hydrocarbon surfaces, although large, are far lower than those on fluorinated surfaces. The largest methylene iodide contact angle on a hydrocarbon surface is only  $77^\circ$  for the  $CH_3$ -rich surface of a single crystal (25); a maximum value of  $71^\circ$  is characteristic of close-packed monolayers of adsorbed aliphatic derivatives (10), showing the sensitivity of  $\theta$  to the packing of the terminal methyl groups.

In Fig. 3a as in Fig. 2a the limiting curve enclosing the data points is found to be a straight line passing through the point  $\cos \theta = 1$  and  $\gamma_{LV} - \gamma_c = 0$ . Since the surface tension of methylene iodide is smaller than that of water, the data point for any given solid surface lies closer to the left side of Fig. 3a than it does in Fig. 2a. But comparison of the two figures reveals that for any given value of  $\gamma_{LV} - \gamma_c$ , the cosine of the methylene iodide contact angle is smaller than that of the water angle; that is, for the same difference between  $\gamma_{LV}$  and  $\gamma_c$ , methylene iodide exhibits a larger contact angle than does water. Since the slope of the limiting straight line is steeper for methylene iodide than for water, the value of  $\gamma_{LV} - \gamma_c$  required for methylene iodide to exhibit a particular contact angle is less than for water. Thus, for a  $90^\circ$  angle, the value of  $\gamma_{LV} - \gamma_c$  required of methylene

iodide needs only to be larger than 34 dynes/cm; this corresponds to a surface with  $\gamma_c < 17$  dynes/cm. In the case of water,  $\gamma_c$  must only be less than 34.6 dynes/cm.

Extrapolation of the limiting straight line for methylene iodide to the maximum possible value of  $\gamma_{LV} - \gamma_c$  indicates a maximum contact angle of 121° for methylene iodide on a hypothetical surface for which  $\gamma_c = 0$ . Thus, although the limiting straight line is steeper than that of water, it terminates before intersecting the  $\cos \theta = -1$  axis and leads to a maximum possible angle of 121°, smaller than that for water.

#### Wetting by n-Hexadecane

In Fig. 5a is a similar plot of  $\cos \theta$  vs  $\gamma_{LV} - \gamma_c$  for n-hexadecane. Fewer data points are included in Fig. 5a than in Figs. 2a or 3a, however, because there are not many low-energy surfaces with critical surface tensions less than the surface tension of hexadecane. In other words, there are relatively few types of surfaces exhibiting nonzero contact angles to hexadecane or other low surface tension oils. On the basis of the data presented in Fig. 1, only two major classes of surfaces can be expected to exhibit substantial oil contact angles: the hydrocarbon surfaces and the fluorine-containing surfaces, provided no other types of halogen atoms are present.

The largest hexadecane angles observed experimentally range from 75° to 78° on surfaces comprising condensed  $-CF_3$  groups; the largest angle (46°) on a hydrocarbon surface is obtained on the analogous  $CH_3$ -surfaces. A straight line is again found (in Fig. 5a) to bound the minimum values of  $\cos \theta$  observed for hexadecane on various solid surfaces. The scatter of the data points relative to this straight line is less than for water or methylene iodide and there is no consistent displacement of open symbols relative to filled symbols (distinguishing between monolayer-coated and bulk surfaces) for atomically comparable surfaces as was observed for the former two liquids.

Only London dispersion force (or induced polarization) interactions with the solid surface are possible for a liquid like hexadecane which has no permanent electric moment and is not capable of hydrogen-bond formation. The data points representing its wetting behavior must therefore lie very close to the straight-line  $\cos \theta$ -vs- $\gamma_{LV}$  relations used to determine the values of  $\gamma_c$  for the different solid surfaces. When such data are transformed to plots of  $\cos \theta$  vs  $\gamma_{LV} - \gamma_c$ , coincidence of the data points at any single value of  $\gamma_{LV} - \gamma_c$  is possible only for those systems having identical  $\cos \theta$ -vs- $\gamma_{LV}$  relations (a common occurrence, to judge from many of the data in Fig. 5a). A second consequence of the transformation is that a straight-line relation between  $\cos \theta$  and  $\gamma_{LV} - \gamma_c$  is possible only if the original  $\cos \theta$ -vs- $\gamma_{LV}$  relations are parallel, the slope of the relation between  $\cos \theta$  and  $\gamma_{LV} - \gamma_c$  being identical to the slopes of the set of parallel relations. Thus, the strong tendency of the data of Fig. 5a to cluster along a single straight line shows how nearly parallel many of the  $\cos \theta$ -vs- $\gamma_{LV}$  relations are, despite wide variations in solid surface composition and physical form. This conclusion is consistent with previous observations (1) that  $\cos \theta$ -vs- $\gamma_{LV}$  curves rarely cross. Moreover, the data points in Fig. 5a tend to cluster toward the lower values of  $\cos \theta$ , indicating that the steeper slopes are the more characteristic for  $\cos \theta$ -vs- $\gamma_{LV}$  relations for the n-alkanes. Another way to say the same thing is that the narrow radial spread of the data in Fig. 5a is indicative of how small or how constant is the interfacial tension  $\gamma_{SL}$  between hexadecane and most low-energy surfaces. This is in contrast with the data for a hydrogen-bonding liquid like water, for example, which show (Fig. 2a) considerable radial divergence.

The slope of the limiting line in Fig. 5a is even steeper than that observed in Fig. 2a for water or in Fig. 3a for methylene iodide. In order for hexadecane to exhibit a contact angle of 90° on a solid surface, the difference between  $\gamma_c$  and  $\gamma_{LV}$  needs only to be larger than 20.8 dynes/cm; however, this corresponds to requiring that the solid surface have a critical surface tension of 6.8 dynes/cm or less. Extrapolation of the linear relation to

its termination at the maximum possible value of  $\gamma_{LV} - \gamma_c$ , which is  $\gamma_{LV}$ , indicates that the largest hexadecane angle possible would be  $109^\circ$  on a hypothetical surface of zero critical surface tension.

#### Wetting by Other Liquids

Similar plots were prepared to the same scale for five additional organic liquids: formamide (Fig. 2b), hexachloropropylene (Fig. 3b), t-butylnaphthalene (Fig. 4a), dicyclohexyl (Fig. 4b), and n-decane (Fig. 5b). Fewer data are available for each of these liquids than for water, methylene iodide, or hexadecane, but the resulting plots all show the same characteristic features. The sequence of graphs in Figs. 2 through 5 is in the order of decreasing surface tension of the reference liquid. This is found to be the same order in which the slope of the limiting straight line becomes steeper; also, it is approximately the order of the decrease in the maximum contact angle possible on a hypothetical surface of zero critical surface tension.

Relatively few data are available for the wetting of low-energy surfaces by liquid metals. Reliable contact angles are available, however, for mercury ( $\gamma_{LV} = 485$  dynes/cm) on three different surfaces. When plotted as a function of  $\gamma_{LV} - \gamma_c$  their data points suggest that a linear limiting relation also characterizes the wetting properties of this liquid metal.

#### LIMITING WETTING BEHAVIOR

The same general pattern in plots of  $\cos \theta$  vs  $\gamma_{LV} - \gamma_c$  appears characteristic of the available data for the nine liquids discussed here. Furthermore, the parameters involved in the straight lines bounding such plots show systematic changes with the surface tension of the reference liquid. Thus, as the surface tension of the reference liquid decreases, the slope of the limiting straight line in these graphs becomes greater. There is a decrease in the value of  $\gamma_{LV} - \gamma_c$  required for a liquid to exhibit any given contact angle (for example,  $\theta = 90^\circ$ ), and the maximum contact angle possible on a hypothetical surface having a value of  $\gamma_c = 0$  tends to become smaller.

The effect of the liquid surface tension on the minimum value of  $\gamma_{LV} - \gamma_c$  required for  $\theta = 90^\circ$  is illustrated in Fig. 6. Each datum point corresponds to a single reference liquid. The data for all nine liquids (from decane with the lowest value of  $\gamma_{LV}$  to mercury

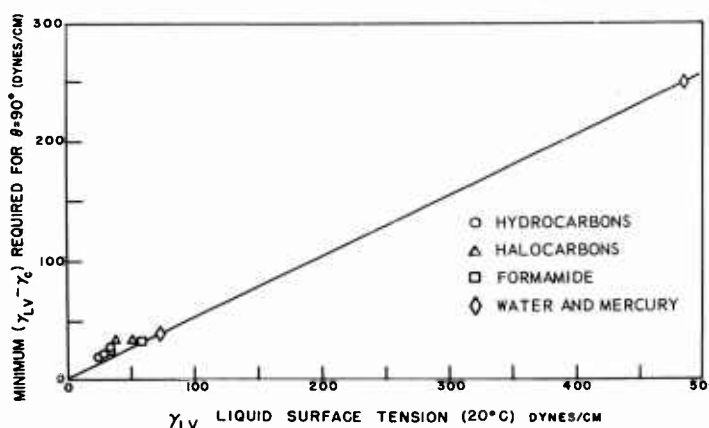


Fig. 6 - Effect of liquid surface tension on a parameter characterizing the limiting wetting behavior

with the highest) plot very close to a straight line passing through the origin at  $\gamma_{LV} = 0$ . This result is remarkable when it is realized that  $\gamma_{LV}$  varies by 25-fold. In no instance among the nine liquids studied was the minimum value of  $\gamma_{LV}-\gamma_c$  required for a  $90^\circ$  contact angle less than half of the surface tension of the liquid; thus, the slope of the line in Fig. 6 is close to, but not quite as low as one-half. From these data there results the following interesting generalization for the design of solid/liquid systems in which capillary penetration is not possible (i.e.,  $\theta \geq 90^\circ$ ): the MINIMUM value of  $\gamma_{LV}-\gamma_c$  which is required to get a  $90^\circ$  contact angle must be more than half of the surface tension of the liquid and therefore the solid must be chosen for which  $\gamma_c$  is less than  $1/2 \gamma_{LV}$ . In Fig. 6 a slight displacement upward (relative to the straight line) is observed for data points for some of the liquids of low  $\gamma_{LV}$ . For these liquids, the minimum difference between  $\gamma_{LV}$  and  $\gamma_c$  required for  $\theta = 90^\circ$  corresponds to a larger fraction of  $\gamma_{LV}$  than that indicated by the slope of the line; this, in turn, indicates a value of  $\gamma_c$  which is proportionately smaller ( $<<1/2 \gamma_{LV}$ ). Since  $\gamma_{LV}$  is already small for these liquids, this restriction introduces a serious limitation, relatively few surfaces being available for which  $\gamma_c$  is of the order of only a few dynes/cm. For example, the data of Fig. 5b for n-decane indicate that, although a maximum contact angle of  $100^\circ$  is possible for a hypothetical surface having  $\gamma_c = 0$ , a solid would require  $\gamma_c < 3.6$  dynes/cm before there was any chance for decane to exhibit a  $90^\circ$  contact angle. The largest angle observed experimentally for decane is  $70^\circ$  on a perfluorolauric acid monolayer with  $\gamma_c = 5.6$  dynes/cm (36).

The maximum contact angle possible on a hypothetical surface having  $\gamma_c = 0$  also shows a marked dependence on  $\gamma_{LV}$  (Fig. 7), increasing rapidly with the surface tension at low values of  $\gamma_{LV}$ , but becoming nearly constant at higher values. From the curve in Fig. 7 a rough estimate can be made of the maximum contact angle possible for a liquid of any given surface tension on the least wettable surface ( $\gamma_c = 0$ ); additionally, it is also possible to indicate the liquids for which a contact angle as large as  $90^\circ$  is not possible, namely, those with surface tensions less than about 20 dynes/cm. To provide an indication of how realistic these maximum contact angles are, there are plotted in Fig. 7 data points corresponding to the largest contact angles observed experimentally at this Laboratory for each liquid on a surface for which critical surface tensions have been determined. These experimental values show the same correlation with  $\gamma_{LV}$  as do the values of the limiting contact angles extrapolated to  $\gamma_c = 0$  although they are invariably smaller since no real surface is available for which  $\gamma_c = 0$ . Examples of real surfaces having critical surface tensions approaching zero are the adsorbed monolayers of fully fluorinated acids (24) which show a linear decrease in  $\gamma_c$  with increasing chain length (N) for homologs through perfluorolauric acid ( $\gamma_c = 5.6$  dynes/cm) (36); if this  $\gamma_c$ -vs-N relation is extrapolated linearly, it intersects the  $\gamma_c = 0$  axis at a value of N corresponding to an acid slightly more than 24 carbon atoms long. Since the  $\cos \theta$ -vs-N data

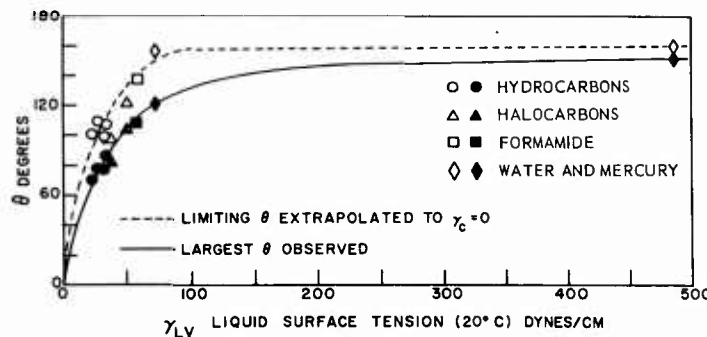


Fig. 7 - Effect of liquid surface tension on the maximum contact angles

for hexadecane on perfluorinated acid monolayers also are essentially linear, they can be extrapolated to the same value of  $N$  and they indicate a maximum contact angle of  $92^\circ$ . This is larger than the  $78^\circ$  observed experimentally on perfluorolauric acid monolayers but is still considerably smaller than the  $109^\circ$  predicted as the limiting angle on a surface of  $\gamma_c = 0$ .

These values are of interest when compared with the contact angles recently reported by Ryan, Kunz, and Shepard (46) for N-ethyl-N-perfluorooctanesulfonylglycine monolayers chemisorbed on the one metal, aluminum. Their hexadecane contact angle of  $110^\circ$  is larger than any previously reported and is close to the limiting maximum indicated in Fig. 7. The same surface, however, exhibited a methylene iodide contact angle of  $160^\circ$ , far above the limiting angle predicted here of  $121^\circ$ . This suggests that although the adsorption experiments were carried out on initially smooth metal surfaces, chemisorption may have resulted in sufficient roughening of the surface to cause enhancement of the observed contact angle in accordance with Wenzel's equation (47). If this is the explanation of the remarkably large apparent contact angles obtained, it indicates that the true angle for hexadecane on a completely smooth surface would still have to exceed  $90^\circ$ .

Relations of the types graphed in Figs. 6 and 7 are suggestive and may prove useful in predicting the limiting wetting behavior of new or unusual liquids. Using the surface tension value for gallium of 735 dynes/cm (48), extrapolation of the graphical relation in Fig. 6 indicates that a minimum value of  $\gamma_{LV} - \gamma_c$  of more than 373 dynes/cm would be required for gallium to exhibit a contact angle of  $90^\circ$ ; this corresponds to a surface for which  $\gamma_c$  needs to be less than 362 dynes/cm. The largest gallium contact angle possible on polyethylene ( $\gamma_c = 31$  dynes/cm) is  $153^\circ$ , while that for Teflon ( $\gamma_c = 18.5$  dynes/cm) is  $157^\circ$ . The maximum possible contact angle on a surface having  $\gamma_c = 0$  is  $163^\circ$ , only slightly larger than that for mercury ( $160^\circ$ ) despite the 50% increase in liquid surface tension.

#### REFERENCES

1. Zisman, W.A., "Relation of Chemical Constitution to the Wetting and Spreading of Liquids on Solids," pp. 30-41 in "A Decade of Basic and Applied Science in the Navy," Office of Naval Research, Report ONR-2, Washington:U.S. Government Printing Office, 1957
2. Shafrin, E.G., and Zisman, W.A., *J. Phys. Chem.* 64:519 (1960)
3. Zisman, W.A., "Relation of the Equilibrium Contact Angle to Liquid and Solid Constitution," *Advances in Chemistry Series*, No. 43, Washington:Am. Chem. Soc., 1963
4. Adam, N.K., and Elliott, G.E.P., *J. Chem. Soc. (London)* 2206 (1962)
5. Kawasaki, K., *J. Colloid Sci.* 17:169 (1962)
6. Baker, H.R., Shafrin, E.G., and Zisman, W.A., *J. Phys. Chem.* 56:405 (1952)
7. Rideal, E., and Tadayon, J., *Proc. Roy. Soc. (London)* A225:346 (1954)
8. Gaines, G.L., Jr., *Nature* 186:384 (1960)
9. Yiannos, P.N., *J. Colloid Sci.* 17:334 (1962)
10. Levine, O., and Zisman, W.A., *J. Phys. Chem.* 61:1068 (1957)
11. "Handbook of Chemistry and Physics," 42nd edit., Cleveland:Chem. Rubber Pub. Co., 1960-61
12. Francis, F., and Piper, S.H., "The Applications of the X-Ray Method to the Study of the Paraffin Hydrocarbons," p. 1203 in "Science of Petroleum Vol. II," Dunstan, A.E., Nash, A.W., Brooks, B.T., and Tizard, H.T., eds., London:Oxford University Press, 1938
13. Kurtz, S.S., Jr., and Sankin, A., "Density and Refractive Index of Hydrocarbons," p. 27 in "Physical Chemistry of the Hydrocarbons, Vol. II," Farkas, A., ed., New York:Academic Press Inc., 1953
14. Stuart, H.A., "Die Struktur des Freien Moleküls," Berlin:Springer-Verlag, 1952
15. London, F., *Trans. Farad. Soc.* 33:8 (1937)
16. Miller, G.A., and Bernstein, R.B., *J. Phys. Chem.* 63:710 (1959)
17. Groves, L.G., and Sugden, S., *J. Chem. Soc. (London)* 1992 (1937)
18. International Critical Tables, 1922
19. Vogel, A.I., *J. Chem. Soc. (London)* 133 (1946)
20. Fox, H.W., Hare, E.F., and Zisman, W.A., *J. Phys. Chem.* 59:1097 (1955)
21. Cottington, R.L., Shafrin, E.G., and Zisman, W.A., *J. Phys. Chem.* 62:513 (1958)

22. Fox, H.W., and Zisman, W.A., *J. Colloid Sci.* 5:514 (1950)
23. Brace, N.O., *J. Org. Chem.* 27:4491 (1962).
24. Shafrin, E.G., and Zisman, W.A., *J. Phys. Chem.* 66:740 (1962)
25. Fox, H.W., and Zisman, W.A., *J. Colloid Sci.* 7:428 (1952)
26. Shafrin, E.G., and Zisman, W.A., *J. Phys. Chem.* 61:1046 (1957)
27. Shafrin, E.G., and Zisman, W.A., *J. Colloid Sci.* 7:166 (1952)
28. Fox, H.W., Hare, E.F., and Zisman, W.A., *J. Colloid Sci.* 8:194 (1953)
29. Ellison, A.H., and Zisman, W.A., *J. Phys. Chem.* 58:503 (1954)
30. Hare, E.F., NRL, private communication
31. Shafrin, E.G., unpublished results
32. Bascom, W.D., and Singleterry, C.R., *J. Phys. Chem.* 65:1683 (1961) and private communication
33. Bennett, M.K., and Zisman, W.A., *J. Phys. Chem.* 63:1241 (1959)
34. Cottington, R.L., Murphy, C.M., and Singleterry, C.R., "Effect of Polar-Nonpolar Additives on Oil-Spreading on Solids, with Applications to Nonspreading Oils," NRL Report 5957, July 25, 1963
35. Bennett, M.K., and Zisman, W.A., *J. Phys. Chem.* 66:1207 (1962)
36. Hare, E.F., Shafrin, E.G., and Zisman, W.A., *J. Phys. Chem.* 58:236 (1954)
37. Schulman, F., and Zisman, W.A., *J. Colloid Sci.* 7:465 (1952)
38. Bennett, M.K., and Zisman, W.A., *J. Phys. Chem.* 65:2266 (1961)
39. Bennett, M.K., and Zisman, W.A., *J. Phys. Chem.* 64:1292 (1960)
40. Ellison, A.H., and Zisman, W.A., *J. Phys. Chem.* 58:260 (1954)
41. Fox, H.W., and Zisman, W.A., *J. Colloid Sci.* 7:109 (1952)
42. Ellison, A.H., Fox, H.W., and Zisman, W.A., *J. Phys. Chem.* 57:622 (1953)
43. Fox, R.B., Jarvis, N.L., Isaacs, L.G., and Zisman, W.A., "Surface Activity at Organic-Liquid/Air Interfaces. Part V - The Effect of Partially Fluorinated Additives on the Wettability of Solid Polymers," NRL Report 5952, July 25, 1963
44. Fox, H.W., and Levine, O., NRL, private communication
45. Ray, B.R., Anderson, J.R., and Scholtz, J.J., *J. Phys. Chem.* 62:1220 (1958)
46. Ryan, J.P., Kunz, R.J., and Shepard, J.W., *J. Phys. Chem.* 64:525 (1960)
47. Wenzel, R.N., *Ind. Eng. Chem.* 28:988 (1936)
48. Mack, G.L., Davis, J.K., and Bartell, F.E., *J. Phys. Chem.* 45:846 (1941)

## UNCLASSIFIED

Naval Research Laboratory. Report 5985.  
UPPER LIMITS FOR THE CONTACT ANGLES OF  
LIQUIDS ON SOLIDS, by Elaine G. Shafrin and  
W.A. Zisman. 22 pp. and figs., September 12, 1963.

Earlier systematic studies of the angle of contact  
( $\theta$ ) exhibited by drops of liquid on plane solid surfaces  
of low surface energy have made data available on  
equilibrium contact angles. These data were obtained  
under well-controlled and comparable experimental  
conditions for many liquids on over 100 different solid  
surfaces. Examination of the data for eight, selected,  
pure liquids (water, formamide, methylene iodide,  
hexachloropropylene, t-butylnaphthalene, dicyclohexyl,  
n-hexadecane, and n-decane) reveals a wide variation  
in the wetting behavior of any single liquid toward  
UNCLASSIFIED (over)

## UNCLASSIFIED

Naval Research Laboratory. Report 5985.  
UPPER LIMITS FOR THE CONTACT ANGLES OF  
LIQUIDS ON SOLIDS, by Elaine G. Shafrin and  
W.A. Zisman. 22 pp. and figs., September 12, 1963.

Earlier systematic studies of the angle of contact  
( $\theta$ ) exhibited by drops of liquid on plane solid surfaces  
of low surface energy have made data available on  
equilibrium contact angles. These data were obtained  
under well-controlled and comparable experimental  
conditions for many liquids on over 100 different solid  
surfaces. Examination of the data for eight, selected,  
pure liquids (water, formamide, methylene iodide,  
hexachloropropylene, t-butylnaphthalene, dicyclohexyl,  
n-hexadecane, and n-decane) reveals a wide variation  
in the wetting behavior of any single liquid toward  
UNCLASSIFIED (over)

## UNCLASSIFIED

Naval Research Laboratory. Report 5985.  
UPPER LIMITS FOR THE CONTACT ANGLES OF  
LIQUIDS ON SOLIDS, by Elaine G. Shafrin and  
W.A. Zisman. 22 pp. and figs., September 12, 1963.

Earlier systematic studies of the angle of contact  
( $\theta$ ) exhibited by drops of liquid on plane solid surfaces  
of low surface energy have made data available on  
equilibrium contact angles. These data were obtained  
under well-controlled and comparable experimental  
conditions for many liquids on over 100 different solid  
surfaces. Examination of the data for eight, selected,  
pure liquids (water, formamide, methylene iodide,  
hexachloropropylene, t-butylnaphthalene, dicyclohexyl,  
n-hexadecane, and n-decane) reveals a wide variation  
in the wetting behavior of any single liquid toward  
UNCLASSIFIED (over)

## UNCLASSIFIED

Naval Research Laboratory. Report 5985.  
UPPER LIMITS FOR THE CONTACT ANGLES OF  
LIQUIDS ON SOLIDS, by Elaine G. Shafrin and  
W.A. Zisman. 22 pp. and figs., September 12, 1963.

Earlier systematic studies of the angle of contact  
( $\theta$ ) exhibited by drops of liquid on plane solid surfaces  
of low surface energy have made data available on  
equilibrium contact angles. These data were obtained  
under well-controlled and comparable experimental  
conditions for many liquids on over 100 different solid  
surfaces. Examination of the data for eight, selected,  
pure liquids (water, formamide, methylene iodide,  
hexachloropropylene, t-butylnaphthalene, dicyclohexyl,  
n-hexadecane, and n-decane) reveals a wide variation  
in the wetting behavior of any single liquid toward  
UNCLASSIFIED (over)

**UNCLASSIFIED**

different solid surfaces. For each liquid, however, graphical plots of cosine  $\theta$  versus the difference in the surface tension ( $\gamma_{lv}$ ) of the pure liquid and the critical surface tension of spreading ( $\gamma_c$ ) of the solid are found to group available data into a zone bounded by a straight line passing through the origin ( $\cos \theta = 1, \gamma_{lv} - \gamma_c = 0$ ). From the parameters defining this straight line, estimates can be made of the limiting contact angles for each liquid. These estimates indicate that the maximum possible contact angle for water is 156°, a value of considerable practical as well as theoretical significance, and that for hexadecane is 109°. The largest values of  $\theta$  obtained experimentally are compared with the maximum values of  $\theta$  as an indication of the extent to which actual systems approach these limiting cases.

A rectilinear relation is found between  $\gamma_{lv}$  and the minimum value of  $\gamma_{lv} - \gamma_c$  required for a surface to exhibit a 90° contact angle; extension of this relation to large values of  $\gamma_{lv}$  provides a good fit to the available data for a pure liquid metal, mercury.

**UNCLASSIFIED**

**UNCLASSIFIED**

different solid surfaces. For each liquid, however, graphical plots of cosine  $\theta$  versus the difference in the surface tension ( $\gamma_{lv}$ ) of the pure liquid and the critical surface tension of spreading ( $\gamma_c$ ) of the solid are found to group available data into a zone bounded by a straight line passing through the origin ( $\cos \theta = 1, \gamma_{lv} - \gamma_c = 0$ ). From the parameters defining this straight line, estimates can be made of the limiting contact angles for each liquid. These estimates indicate that the maximum possible contact angle for water is 156°, a value of considerable practical as well as theoretical significance, and that for hexadecane is 109°. The largest values of  $\theta$  obtained experimentally are compared with the maximum values of  $\theta$  as an indication of the extent to which actual systems approach these limiting cases.

A rectilinear relation is found between  $\gamma_{lv}$  and the minimum value of  $\gamma_{lv} - \gamma_c$  required for a surface to exhibit a 90° contact angle; extension of this relation to large values of  $\gamma_{lv}$  provides a good fit to the available data for a pure liquid metal, mercury.

**UNCLASSIFIED**

**UNCLASSIFIED**

different solid surfaces. For each liquid, however, graphical plots of cosine  $\theta$  versus the difference in the surface tension ( $\gamma_{lv}$ ) of the pure liquid and the critical surface tension of spreading ( $\gamma_c$ ) of the solid are found to group available data into a zone bounded by a straight line passing through the origin ( $\cos \theta = 1, \gamma_{lv} - \gamma_c = 0$ ). From the parameters defining this straight line, estimates can be made of the limiting contact angles for each liquid. These estimates indicate that the maximum possible contact angle for water is 156°, a value of considerable practical as well as theoretical significance, and that for hexadecane is 109°. The largest values of  $\theta$  obtained experimentally are compared with the maximum values of  $\theta$  as an indication of the extent to which actual systems approach these limiting cases.

A rectilinear relation is found between  $\gamma_{lv}$  and the minimum value of  $\gamma_{lv} - \gamma_c$  required for a surface to exhibit a 90° contact angle; extension of this relation to large values of  $\gamma_{lv}$  provides a good fit to the available data for a pure liquid metal, mercury.

**UNCLASSIFIED**